

## Use of harmonic oscillator potential in the analysis of muonic transition energies

K V SUBBA RAO and A A KAMAL

Physics Department, Osmania University, Hyderabad 500 007, India.

MS received 12 April 1980; revised 4 July 1980

**Abstract.** Energy levels:  $1s_{1/2}$ ,  $2p_{1/2}$ ,  $2p_{3/2}$ ,  $3d_{3/2}$ , and  $3d_{5/2}$  of the muon in the spherical nuclei:  $^{120}\text{Sn}$ ,  $^{197}\text{Au}$  and  $^{208}\text{Pb}$  have been calculated under the assumption of harmonic oscillator potential. The levels are corrected for vacuum polarisation. The agreement with experimental values is better than 0.5%. An accurate method of solving the Dirac equation to obtain the energy eigenvalues is outlined. The importance of choosing the 'classical turning point' as the radius for matching the interior and exterior solutions is discussed.

**Keywords.** Muonic atom; harmonic oscillator potential; classical turning point; vacuum polarisation.

### 1. Introduction

Since the pioneering work of Fitch and Rainwater [1953] great progress has been made in the study of muonic atoms which is now an established technique for probing into the electromagnetic structure of the nuclei. This has been made possible owing to the high accuracy achieved by the introduction of solid state detectors and the improved estimates of quantum electrodynamical corrections to the calculated muonic energy levels. In practice the Dirac equation is numerically solved for the potential corresponding to the assumed charge distribution and the parameters are adjusted until the calculated transition energies agree with the experimental values. The quantum electrodynamical corrections, important among which are the vacuum polarisation and Lamb shift corrections, are allowed in the calculations by standard procedures. The x-ray transition energies in muonic atoms are strongly affected by the nuclear size. In a typical heavy muonic atom, an appreciable part of the muon  $1s_{1/2}$  wave function is immersed within the nucleus itself. Consequently, the transition energies for the low lying orbits ( $2p-1s$ ,  $3d-2p$ ) are strongly sensitive to the nuclear charge distribution. Most of the authors have analysed the experimental data by means of a two- or three- parameter Fermi charge distribution. The analysis of muonic transition energies with an analytical function for the charge distribution leads to the estimation of parameters such as  $t$ , the skin thickness and  $C$ , the half-radius as well as the root mean square radius. In all these cases, however, the choice of one specific analytical form for the charge density rather than another is questionable since there are no *a priori* criteria for the choice. The choice of Fermi distribution for medium and heavy nuclei is mainly dictated by the results of the high energy electron scattering experiments, and the parameters are well deter-

mined by electron scattering experiments which involve high momentum transfer rather than by muonic  $x$ -ray measurements. Since only a few muonic transition energies are sensitive to the charge distribution, only a few parameters characterising the charge density can be determined. The two groups ( $3d-2p$ ) and ( $2p-1s$ ) together allow in principle the determination of two independent parameters of the charge density. For medium nuclei ( $Z \lesssim 60$ ) only the root mean square radius is measured, while for heavy nuclei both radius and surface thickness can be determined. When muonic  $x$ -ray data are analysed in terms of the Fermi charge distribution, the result is given in the form of  $Ct$  diagram (Acker *et al* 1966). A wide range of values of  $C$  and  $t$  are permitted, but all these values give the same r.m.s. radius to an accuracy of better than 1%. The crucial question is whether the results from electron scattering and muonic  $x$ -rays are consistent with each other and what quantities can be determined in a model independent way. Elton (1967) showed that for light and medium nuclei ( $12 \leq A \leq 122$ ) the r.m.s. radius is almost model-independent. The agreement, however, becomes less satisfactory for the heavy nuclei. The muonic  $x$ -ray data are consistent with the assumption of constant  $t$  and  $\rho_N$  (the central nucleon density), although these constants are slightly smaller than those found from the electron scattering data (Acker *et al* 1966). This discrepancy might be due to the assumptions involved, such as the constancy of  $t$ . Because of the insensitivity of the results to the parameter  $t$ , it is of great interest to investigate the accuracy attained in the analysis of the muonic  $x$ -ray data under the assumption of uniform charge distribution, since this distribution is a limiting case of Fermi distribution for  $t=0$ . Further, because the uniform model is a lot simpler than the Fermi distribution, computation is relatively easier. Such an analysis has been done earlier by Fitch and Rainwater (1953), and Frati and Rainwater (1962). In fact, assuming a uniform nuclear model with  $R=r_0 A^{1/3}$ , Fitch and Rainwater found the best fit to the experimentally measured  $2p_{1/2}-1s_{1/2}$  transition energy of 6.02 MeV in lead, for the choice  $r_0=1.17$  fm. The experimental energy is, however, 4% higher than the presently accepted value. Even in the work of Frati and Rainwater, the experimentally measured  $2p_{1/2}-1s_{1/2}$  transition energy, which is 5.99 MeV is 4% higher than the currently known value. Further, the mass of the mu-meson used in their calculations is 2% higher than the accepted value. Also, the radiative corrections have not been applied in their work. It has also been pointed out (Christillin *et al* 1979) that non-relativistic calculations of muonic ground state energy level under the assumption of uniform charge distribution agree within 1% of the experimental result. Ofcourse, the fine structure in the higher levels is not resolved.

In the present study, we show that the accuracy can be considerably increased if the calculations are made relativistically. The fine structure in the higher levels is also resolved. Energy levels of the muon, assuming uniform charge distribution, have been evaluated for spherical nuclei Sn, Au and Pb. The levels are corrected for vacuum polarisation.

## 2. Theory

A muon, which is a Dirac particle, and a nucleus, as an extended charge distribution, interact through the well-understood electromagnetic interaction. If a uniform nuclear charge distribution is assumed, the muon experiences a potential of the form

of a simple harmonic oscillator. The energy eigenvalues of the muon in the electrostatic field of the nucleus are obtained by solving the Dirac equation.

Since the muon-nucleus system is not extremely relativistic (Kim 1971), the Dirac equation reduces to a purely radial equation for a two-component wave function with small component  $f$  and large component  $g$ :

$$df/dr = \frac{kf}{r} - \frac{1}{\hbar C} \{W - V(r) - \mu C^2\}g, \quad (1)$$

$$\frac{dg}{dr} = \frac{1}{\hbar C} \{W - V(r) + \mu C^2\}f - \frac{kg}{r} \quad (2)$$

with the normalisation

$$\int_0^{\infty} (f^2 + g^2)dr = 1.$$

Here  $k=(l-j)(2j+1)$ , with  $j$  and  $l$  the total and orbital angular momentum of an eigen state. In equations (1) and (2),  $W=\mu C^2-E$ , where  $W$  is the total energy of the muon, and  $E$  is the binding energy of the muon in the central field  $V(r)$  and  $\mu C^2$  is the rest mass energy corresponding to the reduced mass of the muon.

The energy eigenvalues are obtained by solving the above pair of coupled equations and matching the ratio  $f/g$  for the interior and exterior solutions. This is equivalent to matching the logarithmic derivative of the solution for a second-order differential equation (Barrett 1977).

The Dirac equation has been solved for harmonic oscillator potential

$$V(r) = -\frac{3Ze^2}{2R} + \frac{Ze^2}{2R^3}r^2 \text{ for } r \leq R \quad (3a)$$

$$= -Ze^2/r \text{ for } r \geq R \quad (3b)$$

with  $R = r_0 A^{1/3}$  and  $r_0 = 1.2$  fm.

The general method for solving the Dirac equation, which is due to Barrett (1977), is outlined below.

Set  $W - \mu C^2 = P (= -E)$ ,

$$W + \mu C^2 = Q,$$

$$1/\hbar C = S.$$

Then, equations (1) and (2) respectively become

$$df/dr = \frac{kf}{r} - S[P - V(r)]g, \quad (4)$$

$$dg/dr = S[Q - V(r)]f - \frac{kg}{r}. \quad (5)$$

In order to start the solution near  $r=0$ ,  $V(r)$ ,  $f(r)$  and  $g(r)$  are expanded as power series:

$$V(r) = \sum_{n=0} V_n r^n, \quad (6)$$

$$g(r) = \sum_{m=0} a_m r^{m+s}, \quad (7)$$

$$f(r) = \sum_{m=0} b_m r^{m+t}. \quad (8)$$

It is to be noted that  $s$  and  $t$  are equal for a potential which goes as  $1/r$  and unequal for a finite potential. For  $k < 0$ , the regular solution is given by  $s = -k$ ,  $t = 1 + s$  and  $a_1 = 0$  (Barrett 1977). From (4) to (8), we obtain

$$a_{m+2} = \frac{S \left[ Qb_m - \sum_{n=0}^m V_n b_{m-n} \right]}{(m+2)}, \quad (9a)$$

$$b_m = \frac{S \left[ -Pa_m + \sum_{n=0}^m V_n a_{m-n} \right]}{(m-2k+1)}. \quad (10a)$$

In this case  $a_0$  determines the normalisation. For simplicity it is assumed that  $a_0 = 1$ .

For  $k > 0$ , the regular solution is given by  $t = k$ ,  $s = 1 + t$  and  $b_1 = 0$  (Barrett 1977) and we obtain

$$a_m = \frac{S \left[ Qb_m - \sum_{n=0}^m V_n b_{m-n} \right]}{(m+2k+1)}, \quad (9b)$$

$$b_{m+2} = \frac{S \left[ -Pa_m + \sum_{n=0}^m V_n a_{m-n} \right]}{(m+2)}. \quad (10b)$$

In this case  $b_0$  determines normalisation. Again, it is assumed that  $b_0 = 1$ .

For harmonic oscillator potential,  $V_0 = -3Ze^2/2R$  and  $V_2 = Ze^2/2R^3$  and other coefficients are zero.

To begin with, a value for  $E$  is guessed and the coefficients  $a_m$  and  $b_m$ , and hence the unnormalised values of  $f$  and  $g$  near the origin are calculated. These series solutions are used to start the integration process since the coefficients of  $f$  and  $g$  in the differential equation are infinite at  $r = 0$ . The integration is done

numerically in steps of 0.25 fm by the predictor-corrector-modifier method of Haming. This method is known to be more accurate and stable than other methods such as Milne's, Adam's or Runge-Kutta (Krishna Murthy and Sen 1976; Ralston and Wilf 1960).

The interior solution is regular at  $r=0$  and is obtained by integrating outwards. In order to obtain energy eigenvalues, the interior solution is matched with the exterior solution, which vanishes at  $r = \infty$ . The exterior solution may be obtained for the region outside the nucleus by using a series expansion for the solutions of the Dirac equation for a coulomb potential  $-Ze^2/r$  (Acker *et al* 1966). However, we followed a slightly different and more powerful method in which the numerical integration is carried inwards from the region where  $f$  and  $g$  are negligibly small (Barrett 1977). This procedure facilitates the inclusion of vacuum polarisation correction to the potential that is used in the Dirac equation.

First, the asymptotic solutions for (4) and (5) are obtained. For large  $r$ , (4) and (5) reduce respectively to

$$df/dr = -SPg, \quad (11)$$

$$dg/dr = SQf. \quad (12)$$

The solutions for the above two equations are:

$$g = \exp \{ - (-PQ)^{1/2} Sr \}, \quad (13)$$

$$f = - (-P/Q)^{1/2} g. \quad (14)$$

Starting with these asymptotic values for  $f$  and  $g$  (4) and (5) are integrated inwards from a large value of  $r$ , say 500 fm. The ratio  $f/g$  for the interior and exterior solutions is matched at the 'classical turning point radius' (Barrett 1977), which is found by noting the point where the successive values of  $g''/g$  have opposite signs. The classical turning point is not far from the point which satisfies the relation

$$[P - V(r)] [Q - V(r)] = k(k + 1)/S^2 r^2 \quad (15)$$

If the energy  $E$  of the muon is negative, then there is a point  $r=a$ , beyond which  $(E-V)$  is negative (figure 1); classically, a muon would never reach a radii larger than  $a$ —the classical turning point. Beyond this point, the solutions generally have an exponential behaviour. Hence it is essential that the turning point be chosen as the matching radius to obtain correct results. Only if  $E$  happens to be the eigenvalue, the interior solution will fit a decaying exponential solution exactly. In the case of Dirac equation, the ratio  $f/g$  of the interior and exterior solutions match exactly. It is obvious that the turning point radius increases as  $|E|$  decreases. In case of Pb, the turning point radius occurs for  $1s$  level around 11.25 fm for  $2p$  levels around 23 fm, and for  $3d$  levels around 44 fm. Since  $|E|$  for a particular quantum level decreases as  $Z$  decreases, the corresponding turning point radius is larger. In the case of Sn, it occurs for  $1s$  level around 14 fm, for  $2p$  levels around 34 fm, and for  $3d$  levels around 72 fm. This clearly indicates that it is not correct to fix the match-

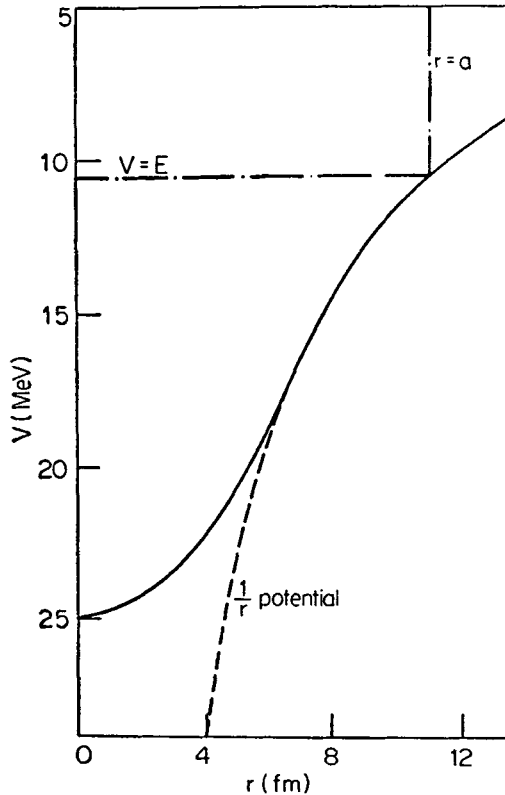


Figure 1. Harmonic oscillator potential with  $R = 7.11$  fm in  $^{208}\text{Pb}$ .  $a$  is the classical turning point radius for  $1s_{1/2}$  level.

ing radius arbitrarily and take the same for all the levels as in the work of Acker *et al* (1967).

The first requirement in finding the exact eigenvalue is to obtain correct number of nodes in the large component  $g$ . If  $n$  is the principal quantum number,  $g$  should contain  $(n-l-1)$  nodes within the turning point radius (Barrett 1977). So, guessing a value for the energy  $E$ , the integration is carried out to the turning point and the number of nodes in the large component  $g$  is observed. The value of  $E$  is then adjusted to get the correct number of nodes. The second requirement in obtaining the exact eigenvalue is to match the ratio  $f/g$  of the interior and exterior solutions at the turning point. After three or four trials, the actual eigenvalue is obtained from interpolation. It is to be noted that in all the trials the integration procedure has to be started from the origin by evaluating the coefficients  $a_m$  and  $b_m$  for each trial energy  $E$ .

### 3. Vacuum polarisation correction

The electrostatic field of the nucleus induces a slight separation of virtual electron-positron pairs—a quantum electrodynamical phenomenon referred to as vacuum polarisation. The vacuum polarisation changes the electrostatic potential of the nucleus and this effect is felt upto a distance of the order of compton wavelength of

the electron ( $\approx 10^{-11}$  cm). Since the muon spends a greater fraction of time within this distance, it experiences on an average, a nuclear charge larger than the asymptotic value at large distances. This always increases the force between the nucleus and the muon leading to an increase in the binding energy of the muon. The vacuum polarisation correction is about two orders of magnitude larger than experimental errors and hence cannot be ignored.

The main contribution to the polarisation is from monopole field, and its effect is equivalent to an additional field  $V_{VP}(r)$  (Engfer *et al* 1974) given by

$$V_{VP}(r) = -\frac{2}{3} \alpha e^2 \lambda \int_0^\infty dr' \frac{r'}{r} \left[ H(|r-r'|) - H(r+r') \right] \rho(r'), \quad (16)$$

$$H(r) = \int_1^\infty \frac{dy}{y^2} \exp(-2yr/\lambda) \left(1 + \frac{1}{2y^2}\right) \left(1 - \frac{1}{y^2}\right)^{\frac{1}{2}}, \quad (17)$$

where  $\lambda (= \hbar/m_e c)$  is the reduced compton wavelength of the electron. If the above integral is evaluated numerically, the computer time consumed is very large. In order to save the computer time, the integral is expanded as a power series in  $(r/\lambda)$  (Barrett 1977). The expansion given by Barrett (1977) is accurate only if  $r/\lambda < 1/3$ . An expansion to higher powers of  $(r/\lambda)$  is given by McKinley (Engfer *et al* 1974). This expansion gives sufficiently accurate values of  $H(r)$  upto  $r \lesssim \lambda$  and is given below.

$$\begin{aligned} H(r) = & \frac{9\pi}{32} + \frac{2r}{\lambda} \left\{ \left( \gamma + \ln \frac{r}{\lambda} \right) \left[ 1 - \left( \frac{r}{\lambda} \right)^4 \left( \frac{1}{20} + \frac{1}{630} (r/\lambda)^2 \right) \right. \right. \\ & \times \left. \left. \left( 1 + \frac{1}{32} (r/\lambda)^2 \left[ 1 + \frac{4}{165} (r/\lambda)^2 \right] \right) \right] - \frac{1}{6} - \pi(r/\lambda) \right. \\ & \times \left( \frac{3}{8} + \frac{1}{12} (r/\lambda)^2 \right) + \frac{1}{2} (r/\lambda)^2 \left[ 1 + \frac{1}{150} (r/\lambda)^2 \right. \\ & \times \left( 38 + \frac{1}{882} (r/\lambda)^2 \left( 949 + \frac{1}{96} (r/\lambda)^2 \right) \right. \\ & \left. \left. \left. \left. \times \left( 2987 + \frac{138778}{1815} (r/\lambda)^2 \right) \right) \right] \right\} \end{aligned} \quad (18)$$

where  $\gamma = 0.5772157$ ,  $\lambda = 386.15915$  fm and  $1/\alpha = 137.03602$ . Applying (16) to the case of uniform charge distribution we finally obtain

$$V_{VP}(r) = \frac{\alpha \lambda Z e^2}{2\pi r R^3} \int_0^\infty dr' r' \left[ H(|r-r'|) - H(r+r') \right]. \quad (19)$$

In evaluating the eigenvalues,  $V_{VP}(r)$  is added to  $V(r)$  before the Dirac equation is solved.

In the case of lead, vacuum polarisation increases the binding energy of  $1s_{1/2}$  level by about 56 keV;  $2p$  levels by about 29 keV;  $3d$  levels by about 9 keV. It is remarkable that these values fairly agree with the corresponding values obtained by Barrett (1977) for Fermi charge density.

The correction due to Lamb shift is very much smaller compared to the correction due to vacuum polarisation. It is about 3 keV for  $1s_{1/2}$  level in lead (Barrett 1977) and much smaller for other levels. Hence, we have neglected it in our calculations.

#### 4. Results and conclusions

The energy levels:  $1s_{1/2}$ ,  $2p_{1/2}$ ,  $2p_{3/2}$ ,  $3d_{3/2}$  and  $3d_{5/2}$  calculated for  $^{120}\text{Sn}$ ,  $^{197}\text{Au}$  and  $^{208}\text{Pb}$  are given in table 1. For comparison, the theoretical values obtained by Barrett (1977) for Fermi charge distribution are also given in the same table. In almost all the cases, the harmonic oscillator energy levels agree with their values within 0.5%. Our value of  $1s_{1/2}$  level in  $^{208}\text{Pb}$  is in much better agreement than the non-relativistic value (10.42 MeV) obtained by Christillin *et al* (1979). The energies for a few transitions derived for harmonic oscillator potential are given in table 2, along with the experimental values taken from the work of Engfer *et al* (1974). In almost all the cases, the  $2p$ - $1s$  transition energies agree with experimental values within 1%; the  $3d$ - $2p$  transition energies within 0.5%. The  $2p$ - $1s$  transition energies for harmonic oscillator potential are underestimated for Pb and Au, whereas they are overestimated for Sn. But, the  $3d$ - $2p$  transition energies are overestimated in all the three elements. This tendency suggests that the uniform charge radius may not have a simple  $A^{1/3}$  dependence as assumed and that the value of  $r_0$ , which has been assumed to be 1.2 fm, is not a constant. The  $2p$  level splitting is overestimated in all the three elements by 5%, thereby indicating that harmonic oscillator potential may not be capable of revealing the exact splitting. The results also suggest that only  $1s_{1/2}$ ,  $2p_{1/2}$  and  $2p_{3/2}$  levels, particularly the first two, are rather sensitive to the nature of the nuclear charge distribution.

For comparison, the coulomb potential generated by the Fermi charge density in  $^{208}\text{Pb}$  with  $C=6.641$  fm and  $t=2.344$  fm. the best values of the parameters obtained by Barrett (1977), is shown in figure 2 along with the harmonic oscillator potential with  $R=7.11$  fm used in our calculations. Although the corresponding charge distributions for these two models are considerably different, the potentials are remarkably similar (figure 2). At the origin the potential due to the Fermi charge density is only 690 keV deeper than the harmonic oscillator potential, but coincides with the  $1/r$  potential around 9 fm. This suggests that for a slight change in the charge distribution, the corresponding change in the potential is much smaller. It has been pointed out by Ford and Willis (1969) that a number of different charge distributions can give rise to the same transition energy. From this it follows that the potentials generated by those different charge distributions be the same. This is understandable since it is the potential rather than the charge density that directly enters the evaluation of energy levels.

Calculations of muonic energy levels for harmonic oscillator potential in other spherical nuclei are in progress, and the sensitivity of the energy levels to the choice of  $r_0$  is also being investigated.

Table 1. Energy levels (keV).

Level	<sup>208</sup> Pb		<sup>197</sup> Au		<sup>180</sup> Sn	
	Calculated for harmonic oscillator potential with $R=7.11$ fm	Calculated for Fermi density <sup>(a)</sup>	Calculated for harmonic oscillator potential with $R=6.98$ fm	Calculated for Fermi density <sup>(a)</sup>	Calculated for harmonic oscillator potential with $R=5.92$ fm	Calculated for Fermi density <sup>(a)</sup>
1s <sub>1/2</sub>	10551.58	10596.51	10078.32	10078.57	5245.77	5220.33
2p <sub>1/2</sub>	4824.21	4813.78	4499.96	4486.02	1818.29	1814.10
2p <sub>3/2</sub>	4632.09	4628.41	4320.17	4316.42	1770.64	1768.44
3d <sub>5/2</sub>	2172.22	2172.93	2012.61	2012.81	792.50	792.20
3d <sub>3/2</sub>	2129.41	2130.11	1975.52	1975.76	786.53	786.24

<sup>(a)</sup> Taken from Barrett (1977).

Table 2. Transition energies (keV).

Transition	<sup>208</sup> Pb		<sup>197</sup> Au		<sup>186</sup> Sn	
	Calculated for harmonic oscillator potential with $R=7.11$ fm	Experimental <sup>(a)</sup>	Calculated for harmonic oscillator potential with $R=6.98$ fm	Experimental <sup>(a)</sup>	Calculated for harmonic oscillator potential with $R=5.92$ fm	Experimental <sup>(a)</sup>
$2p_{1/2}^{-1}1s_{1/2}$	5727.37	5777.91(40)	5578.36	5594.97(70)	3427.48	3408.79(37)
$2p_{3/2}^{-1}1s_{1/2}$	5919.49	5962.77(42)	5758.19	5764.89(70)	3475.13	3454.41(33)
$3d_{3/2}^{-1}2p_{1/2}$	2651.99	2642.11( 4)	2487.35	2474.22(45)	1025.79	1022.20(20)
$3d_{5/2}^{-1}2p_{3/2}$	2459.87	2457.20(20)	2307.56	2304.44(45)	978.14	976.55(30)
$3d_{5/2}^{-1}2p_{5/2}$	2502.68	2500.33( 4)	2344.65	2341.21(45)	984.11	982.20(20)
$\Delta p$	192.12	184.86	179.83	169.92	47.65	45.62
$\Delta d$	42.81	43.13	37.09	36.0	5.97	5.65

<sup>(a)</sup>Taken from Engfer *et al* (1974).

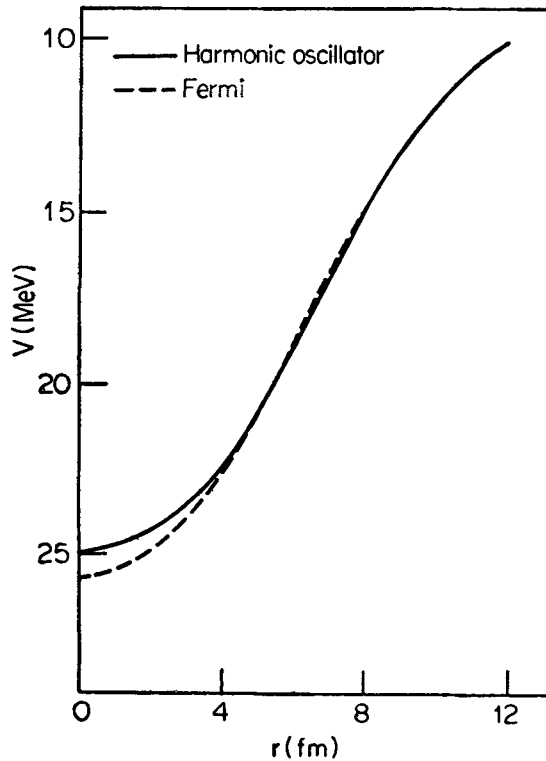


Figure 2. Harmonic oscillator potential with  $R = 7.11$  fm and the potential generated by the Fermi charge distribution in  $^{208}\text{Pb}$ .

### Acknowledgements

One of us (KVS) would like to thank the Council of Scientific and Industrial Research, New Delhi for financial support.

### References

- Acker H L, Backenstoss G, Daum C, Sens J C and DeWitt S A 1966 *Nucl. Phys.* **87** 1  
 Barrett R C 1977 *Muon physics* eds. V W Hughes and C S Wu (New York: Academic Press) Vol. 1, p. 309  
 Christillin P, Rosa Clot M and Servadio S 1979 Ref. Th. 2659—CERN  
 Elton L R B 1967 *Electromagnetic sizes of nuclei* Proc. Int. Conf., Ottawa, D J Brown, p. 267  
 Engfer R, Schneuwly H, Vuilleumier J L, Walter H K and Zehnder A 1974 *Atomic data and nuclear data tables* **14** 509  
 Fitch V L and Rainwater J 1953 *Phys. Rev.* **92** 789  
 Ford K W and Willis J G 1969 *Phys. Rev.* **185** 1429  
 Frati W and Rainwater J 1962 *Phys. Rev.* **128** 2360  
 Kim Y N 1971 *Mesic atoms and nuclear structure* (Amsterdam; North Holland) p. 16  
 Krishna Murthy E V and Sen S K 1976 *Computer-based numerical algorithms* (New Delhi: Affiliated East-West) Chap. 8, p. 340  
 Ralston A R and Wilf H S 1960 *Mathematical methods for digital computers* (New York: John Wiley) p. 95